Small (≤2 cm) hepatocellular carcinoma in patients with chronic liver disease: comparison of gadoxetic acid-enhanced 3.0 T MRI and multiphasic 64-multirow detector CT

J HWANG, MD, S H KIM, MD, M W LEE, MD and J Y LEE, MD

Department of Radiology and Center for Imaging Science, Samsung Medical Center, Sungkyunkwan University School of Medicine, Seoul, Republic of Korea

Objectives: To compare the diagnostic performance of gadoxetic acid-enhanced MRI using 3.0 T with that of multiphasic 64-multirow detector CT (MDCT) for the detection of small (≤2 cm) hepatocellular carcinoma (HCC) in patients with chronic liver disease.
Methods: A total of 54 patients (44 men, 10 women; age range, 33–81 years) with 59 HCCs (≤2 cm in diameter) who underwent both multiphasic (arterial, portal venous, equilibrium) 64-MDCT and gadoxetic acid-enhanced 3.0 T MRI were enrolled in this study. Two observers independently and randomly reviewed the MR and CT images on a lesion-by-lesion basis. The diagnostic performance of these techniques for the detection of HCC was assessed by alternative free-response receiver operating characteristic (ROC) analysis, in addition to evaluating the sensitivity and positive predictive value.
Results: For each observer, the areas under the ROC curve were 0.874 and 0.863 for MRI, respectively, as opposed to 0.660 and 0.687 for CT, respectively. The differences between the two techniques were statistically significant for each observer ($p<0.001$). The sensitivities (89.8% and 86.4%) of MRI for both observers were significantly higher than those (57.6% and 61.0% for each observer, respectively) of MDCT. No significant difference was seen between the positive predictive values for the two techniques ($p>0.05$).
Conclusion: Gadoxetic acid-enhanced 3.0 T MRI shows a better diagnostic performance than that of 64-MDCT for the detection of small (≤2 cm) HCCs in patients with chronic liver disease.

Received 10 September 2010
Revised 14 February 2011
Accepted 23 March 2011

DOI: 10.1259/bjr/27727228

Hepatocellular carcinoma (HCC) is associated with underlying chronic liver disease in more than 90% of cases, and constitutes the leading cause of death in patients with chronic liver disease [1, 2]. Therefore, early detection and accurate assessment of small HCC are of great importance when planning the most appropriate therapeutic approach. The efficacy of various treatments and the survival of patients with small HCC are much more successful than those for patients with larger tumours. The typical imaging feature of HCC on one or two dynamic studies, including either CT scanning, contrast-enhanced ultrasound or MRI, has been used to establish the diagnosis of HCC according to the size of the lesion (1–2 cm or >2 cm in diameter) in patients with chronic liver disease [3, 4]. With a state-of-the-art imaging technique, the detection of smaller lesions in the liver may be possible. However, there is still great difficulty in the characterisation of hypervascular nodules <2 cm in diameter, which often have non-specific imaging characteristics [5].

Address correspondence to: Dr Seong Hyun Kim, Department of Radiology, Samsung Medical Center, Sungkyunkwan University School of Medicine 50, Ilwon-dong, Gangnam-gu, Seoul 135-710, Republic of Korea. E-mail: kshyun@skku.edu

The use of multirow detector CT (MDCT), which has advantages that include greater speed, thinner slices and multiphasic scanning, has improved the chance of detecting HCC [6, 7]. The diagnostic performance of liver MRI for detecting and characterising focal hepatic lesions has also been improved with the development of MRI technologies and MR contrast media [8, 9]. Recently, a widely used liver-specific contrast agent, gadolinium ethoxybenzyl diethylenetriamine pentaacetic acid (gadoxetic acid disodium; Primovist, Bayer Schering Pharma, Berlin, Germany) has produced both dynamic and liver-specific hepatobiliary MR images. This contrast agent is highly liver specific with approximately 50% of the injected dose taken up by functioning hepatocytes and excreted in bile, which enables hepatobiliary phase imaging to start at 10–20 min post injection, and hence makes it more suitable for use in clinical practice [10–12]. On the other hand, another gadolinium-based hepatobiliary agent, gadobenate dimeglumine (Gd-BOPTA/Dimeg; Multihance, Bracco, Milan, Italy), has approximately 3–5% of the injected dose taken up by functioning hepatocytes and excreted in bile, and enables hepatobiliary phase imaging to start at more than 60 min. However, a previous study [13] demonstrated that the diagnostic performance of gadoxetic acid-enhanced MRI and gadobenate dimeglumine-enhanced MRI for

pre-operatively detecting HCC is quite similar. In addition to liver-specific contrast agent, high-field-strength (3.0 T) MRI may possibly be better than 1.5 T due to the advantages of greater signal-to-noise ratio (SNR) and image quality than 1.5 T MRI, thus improving lesion detection (although there are substantial challenges with 3 T in abdominal imaging). The purpose of this study was to compare the diagnostic performance of gadoxetic acid-enhanced MRI using 3.0 T with that of triple-phase 64-MDCT for the detection of small (≤2 cm in diameter) HCC in patients with chronic liver disease.

Methods and materials

Patient selection

This study was conducted with the approval of our institutional review board and informed consent was waived for this retrospective study.

Between April 2008 and October 2008, among a total of 302 consecutive patients with chronic liver disease and suspected HCC on the basis of their imaging findings and/or elevated serum α-fetoprotein level, one study coordinator with 10 years of experience in abdominal imaging retrospectively collected patients with the following criteria: (1) chronic liver disease with focal hepatic lesions with diameters 2 cm or smaller and with a confirmative diagnosis; (2) the patient had undergone both a multiphasic 64-MDCT and a gadoxetic acid-enhanced MRI using 3.0 T within 1 month because of a suspicion of new HCC based on previous imaging and/or clinical findings, including increased serum α-fetoprotein level; and (3) the patient had undergone a follow-up CT and/or MRI after 1 year or longer. A total of 54 patients (44 males, 10 females; age range, 33–81 years) with 59 HCCs (mean, 1.2 cm; range, 0.5–2.0 cm; diameter ≤1 cm, 28 HCCs; 1 cm <diameter ≤2 cm, 31 HCCs) fitted these criteria and were included in this study. 24 of the 54 patients had 1 HCC, 6 patients had 2 HCCs, 6 patients had 3 HCCs and 1 patient had 5 HCCs. The other 17 patients had no HCC, but had nodules with iodised-oil accumulation, dysplastic nodules and nodular arterial enhancing pseudolesions such as arterioportal shunt. Among them, 4 patients had a previous history of surgery for HCC and 19 patients had previous locoregional therapy such as TACE (transcatheter arterial chemoembolisation) or RFA (radiofrequency ablation) for HCC. The diagnosis of HCC was made by histopathological confirmation following surgical resection (n=6) or by percutaneous biopsy (n=2). The diagnosis of 51 HCC was made according to (1) new hypervascular focal liver lesion compared with previous triple-phase MDCT or gadoxetic acid-enhanced MRI performed for the surveillance of HCC in patients with chronic liver disease and characteristic angiographic findings of HCC, followed by sustained iodised oil accumulations in the nodule on follow-up CT after TACE [3, 14, 15] (n=49); and (2) the combination of a characteristic enhancement pattern of HCC (hypervascular at arterial phase and washout at portal or equilibrium phase) on multiphasic MDCT and gadoxetic acid-enhanced MRI and the increase in lesion size on follow-up imaging (n=2). In all patients, the diagnosis of liver cirrhosis was made according to the pathology findings (n=9) or a combination of the radiological and clinical findings as well as the results of laboratory examinations, including blood chemistry tests (n=45). Underlying liver cirrhosis was associated with viral hepatitis B in 38 patients, viral hepatitis C in 10 patients, alcoholic cirrhosis in 1 patient, Wilson disease in 1 patient and unknown cause in 4 patients.

Imaging methods

Multiphasic (contrast-enhanced hepatic arterial, portal venous and equilibrium phases) CT was conducted with a 64-MDCT scanner (Aquilion 64, Toshiba Medical, Ottawara, Japan; and Lightspeed VCT 64, GE Healthcare, Little Chalfont, UK). The scanning parameters were as follows: 120 kVp, 189–200 mAs, 5 mm slice thickness with an increment (overlap) of 2.5 mm, table speed of 26.5–39.37 mm rotation^{-1} (pitch, 0.828–1.07), and a single-breath-hold helical acquisition time of 4–6 s, depending on liver size. Images were obtained in the craniocaudal direction. Hepatic arterial phase scanning began 30–40 s after the injection of 120 ml of a non-ionic iodinated contrast agent (iopamidol; Iopamiro 300, Bracco) at a rate of 3–4 ml s^{-1} via a bolus-triggered technique (120 kVp; 40–60 mA; monitoring frequency from 12 s after the contrast injection, 1 s; trigger threshold, 100 HU in the descending aorta; delay from trigger to initiation of scan, 18 s). The contrast agent was administered through the antecubital vein with a power injector. The portal and equilibrium phases of scanning began 70 and 180 s after the injection of the contrast agent, respectively.

MRI was conducted using a 3.0 T whole-body MRI system (Intera Achieva 3.0 T; Philips Healthcare, Best, the Netherlands) with a 16-channel phased-array coil as the receiver coil. The liver was imaged in the axial plane in all patients, both prior to and after the administration of gadoxetic acid at a dose of 0.1 ml kg^{-1} (0.25 mmol ml^{-1}). The contrast agent was administered through the antecubital vein with a power injector at a rate of 2 ml s^{-1}, followed by a 20 ml saline flush.

The MRI protocol included a respiration-triggered T_1 weighted turbo field-echo in-phase sequence (repetition time/echo time, 10/2.3; flip angle, 15°; matrix size, 288 × 230; bandwidth, 434.3 Hz pixel^{-1}) and an out-of-phase sequence (10/3.45; flip angle, 15°; matrix size, 288 × 230; bandwidth, 434.3 Hz pixel^{-1}), a respiration-triggered single-shot T_2 weighted sequence with a reduction factor of 2 or 4 (1342/80; flip angle, 90°; matrix size, 320 × 256; bandwidth, 506.4 Hz pixel^{-1}), a breath-hold multishot T_2 weighted sequence with a reduction factor of 2 or 4 (2161/70; flip angle, 90°; matrix size, 400 × 280; bandwidth, 235.2 Hz pixel^{-1}), a respiration-triggered single-shot heavily T_2 weighted sequence with a reduction factor of 2 or 4 (1573/160; flip angle, 90°; matrix size, 320 × 256; bandwidth, 317.9 Hz pixel^{-1}) with a section thickness of 5–7 mm, an intersection gap of 1–2 mm and a field of view of 32–38 cm. For gadoxetic acid-enhanced MRI, unenhanced, arterial phase (20–35 s; via a bolus-triggered technique under fluoroscopic guidance), portal phase (60 s), late phase (3 min), and 20-min delayed hepatobiliary phase images were obtained with a T_1 weighted three-dimensional turbo-field-echo sequence

(T_1 high-resolution isotropic volume examination; THRIVE, Philips Healthcare; 3.4/1.8; flip angle, 10°; matrix size, 336 × 206; bandwidth, 995.7 Hz pixel^{-1}) with a section thickness of 2 mm and a field of view of 32–38 cm.

Image analysis

Two blinded gastrointestinal radiologists with at least 5 years of experience in the interpretation of CT/MR images of the liver independently and randomly reviewed the CT and MR images. The observers knew that the patients were at risk of HCC, but did not know the patient history, laboratory results, findings of other imaging modalities or the final diagnosis. The interval between reviews of the CT and MR images was at least 1 month. All images were evaluated with a 2000 × 2000 PACS (GE Healthcare) monitor with adjustment of the optimal window setting in each case. Each observer independently recorded the presence and segmental location of the lesions using a 4-point confidence scale to assign a confidence level to each lesion. The confidence level was defined as follows: 1, probably not an HCC; 2, a possible HCC; 3, a probable HCC; 4, a definite HCC. Upon review of the image, the observers were aware that sensitivity was calculated with the number of lesions assigned a confidence level of 3 or 4. In clinical practice at our institution, nodules that became enhanced in the arterial phase and had a washout pattern in the portal or equilibrium phase with or without capsular enhancement at triple-phase MDCT were considered HCC [4, 16–19]. The criteria for HCC on gadoxetic acid-enhanced MR images were similar to the criteria for the triple-phase dynamic CT pattern: enhancement in the arterial phase and a washout pattern in the portal or 3-min late phase that revealed the mixed enhancing features of both equilibrium phase and hepatobiliary phase images as hepatocyte-related enhancement starts approximately 1 min after intravenous injection of gadoxetate disodium [20]. In addition to the foregoing features, a hypointense nodule seen on the gadoxetic acid-enhanced 20-min delayed hepatobiliary phase MR images was considered HCC on the basis of previous findings [11]. A hypervascular nodule seen on gadoxetic acid-enhanced arterial phase MR images with a washout pattern was considered HCC even though the nodule appeared isointense or hyperintense on hepatobiliary phase images [11]. We also made reference to unenhanced images (T_1, T_2 weighted image), in addition to the criteria. To avoid a mismatch between the findings on the scored lesions and the findings with the standard of reference for determining the total number of lesions, each observer recorded the individual image number, the segmental location of all lesions and the size of each lesion. For patients with two or more lesions in one segment, detailed descriptions of the location of the lesion in each segment were added in order to avoid confusion in the data analysis. After the two observers had completed the review, the study coordinator and two observers compared the scoring results of each observer with the reference standard, and devised a possible explanation for the causes of false positive and false negative findings with the consensus.

Statistical analysis

On the basis of the two observers' reviews, an alternative free-response receiver operating characteristic (ROC) analysis was generated on a lesion-by-lesion basis. The diagnostic performance of each technique for each observer was assessed by measuring the area under the ROC curve (Az), in accordance with the methods published by Hanley and McNeil [21]. The sensitivity of each observer and technique used for the detection of HCC was calculated. The true-positive lesions were identified as having assigned confidence levels of 3 or 4 by the observers and proven to be HCC. False-positive lesions were those assigned confidence levels of 3 or 4 that were confirmed to be benign lesions, and false-negative lesions were those assigned confidence levels of 1 or 2 that were confirmed to be HCC. The difference in the sensitivity was statistically analysed via McNemar's test. The statistical analysis of differences in the calculated positive predictive values for each observer and technique were based on a previous report [22]. A value of $p<0.05$ was considered statistically significant. An analysis of all false-positive and false-negative observations was also undertaken. Kappa statistics were used to evaluate the degree of agreement between the two observers with each technique and was categorised as follows: κ-values of 0.00–0.20 were considered indicative of poor agreement; 0.21–0.40, fair agreement; 0.41–0.60, moderate agreement; 0.61–0.80, good agreement; and 0.81–1.00, excellent agreement [23].

Results

Table 1 shows the Az values for each observer and for each technique. For both observers, MRI achieved significantly higher Az values than those of CT ($p<0.001$). The MR sensitivities of all observers for the detection of HCCs were significantly higher than the CT sensitivities ($p<0.001$; Table 2; Figure 1). The differences in the positive predictive values between MRI and CT for the

Table 1. Area under the receiver operating characteristics curve (Az) for gadoxetic acid-enhanced MRI and multiphasic multirow detector CT (MDCT) for the detection of small (≤2 cm) hepatocellular carcinomas in patients with chronic liver disease

Technique	Observer 1	Observer 2
Gadoxetic acid-enhanced MRI	0.874 ± 0.032 (0.807, 0.925)	0.863 ± 0.033 (0.794, 0.916)
MDCT	0.660 ± 0.047 (0.575, 0.739)	0.687 ± 0.046 (0.602, 0.764)
Difference in Az	0.214 ± 0.053	0.176 ± 0.049

Values are Az ± one standard error. The differences in Az of the two techniques for each observer are statistically significant ($p<0.001$). Data in parentheses are 95% confidence intervals.

Table 2. Diagnostic predictive values of gadoxetic acid-enhanced MRI and multiphasic multirow detector CT (MDCT) in the detection of small (≤2 cm) hepatocellular carcinomas in patients with chronic liver disease

Technique	Observer 1	Observer 2
Sensitivity per lesion (%)		
Gadoxetic acid-enhanced MRI	89.8 (53)	86.4 (51)
MDCT	57.6 (34)	61.0 (36)
Positive predictive value (%)		
Gadoxetic acid-enhanced MRI	88.3 [53/60] (7)	94.4 [51/54] (3)
MDCT	91.9 [34/37] (3)	94.7 [36/38] (2)

Numbers in parentheses in sensitivity and positive predictive values are the numbers of true-positive and false-positive lesions, respectively. For positive predictive value, numbers in brackets are the number of true-positive lesions divided by the total number of lesions assigned confidence levels of 3 or 4.

The sensitivities of the two techniques for each observer were significantly different ($p<0.001$). The positive predictive values of the two techniques for each observer were not significantly different ($p>0.05$).

two observers were not significantly different ($p>0.05$). In the detection of HCC ≤1 cm in diameter, all observers had significantly higher sensitivities with MRI than with CT ($p<0.05$; Table 3; Figure 2). For the detection of HCC >1 cm, the sensitivities between the two techniques for all observers were not significantly different ($p>0.05$).

Among the 59 HCCs, an HCC of 0.6 cm diameter was not identified by all observers on both CT and MRI,

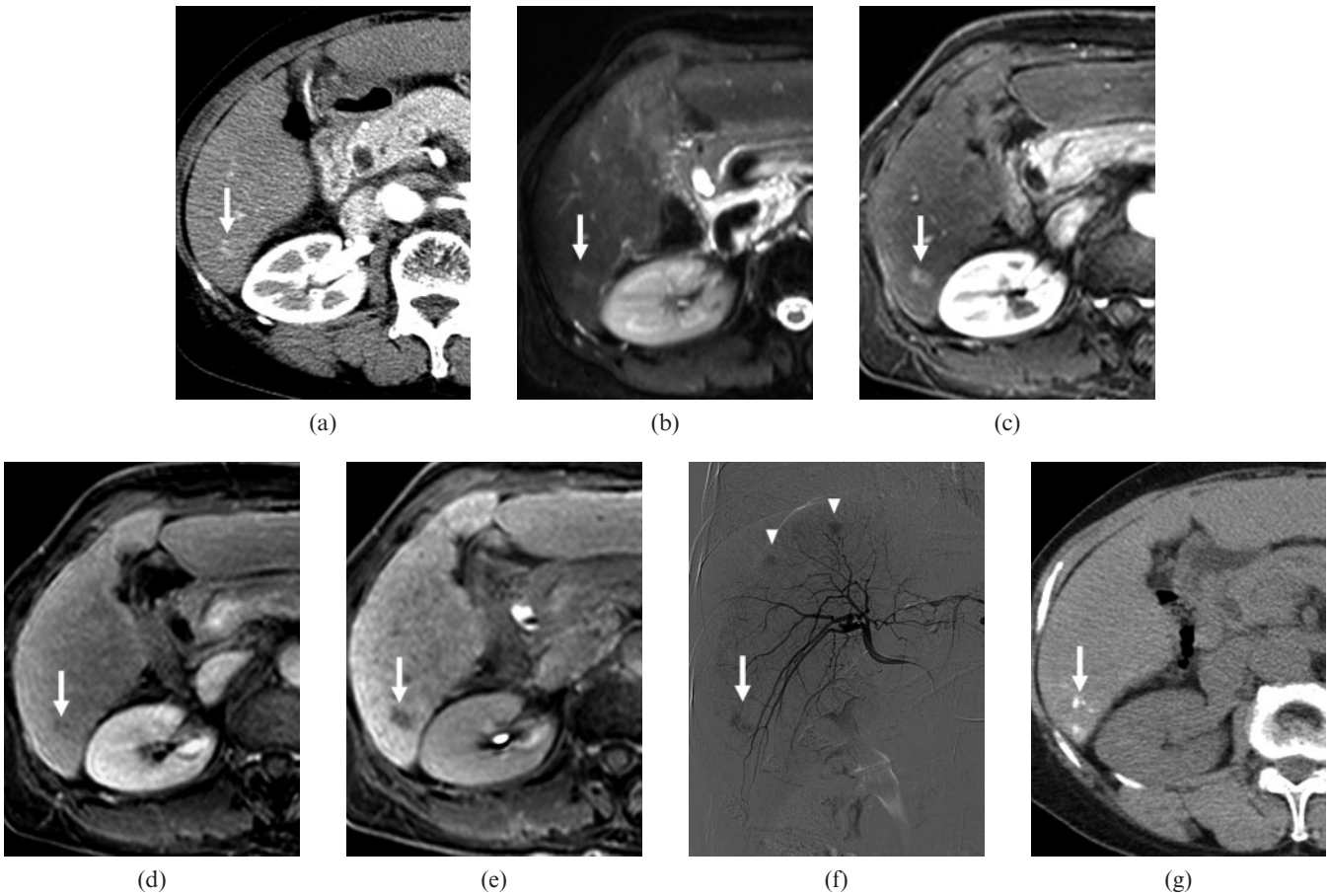

Figure 1. A 68-year-old female with three (1.1, 2.3 and 2.5 cm in diameter) hepatocellular carcinomas (HCCs). (a) Contrast-enhanced CT scan obtained on arterial phase shows a faint enhancing nodule of 1.1 cm diameter with poor conspicuity in segment VI (arrow). The nodule showed no washout pattern on equilibrium phase (not shown). All observers interpreted the nodule as arterioportal shunt. (b) T_2 weighted MR image shows a hyperintense nodule in segment VI (arrow). (c) Gadoxetic acid-enhanced arterial phase MR image shows a hypervascular nodule in segment VI (arrow). (d) Gadoxetic acid-enhanced 3-min late phase MR image shows the nodule with a washout pattern in segment VI (arrow). (e) Gadoxetic acid-enhanced hepatobiliary phase MR image shows a hypointense nodule in segment VI (arrow). All observers interpreted the nodule as HCC. (f) Right hepatic angiography shows a hypervascular tumour staining in segment VI (arrow). Other hypervascular tumour staining is also observed (arrowhead). (g) Unenhanced CT scan obtained after transcatheter arterial chemoembolisation shows iodised-oil accumulation at the corresponding HCC (arrow).

Table 3. Sensitivity of gadoxetic acid-enhanced MRI and multiphasic multidetector row CT for the detection of hepatocellular carcinomas (HCCs) according to tumour size

		Observer 1		Observer 2	
Tumour diameter, *D* (cm)	Total	MRI	CT	MRI	CT
$D \leq 1$	28	25 (89)	6 (21)	22 (79)	9 (32)
$1 < D \leq 2$	31	28 (90)	28 (90)	29 (94)	27 (87)

Numbers are the numbers of HCCs. Numbers in parentheses are the percentages. For the detection of HCCs ≤1 cm in diameter, all observers had higher sensitivity with MRI than with CT ($p<0.05$). For the detection of HCCs >1 cm, the sensitivities between two techniques for all observers were not significantly different ($p>0.05$).

which was attributed to faint enhancement with no washout on CT, and a small size despite the typical enhancement pattern of HCC on MR images in a retrospective review. 16 HCCs (mean tumour size, 0.8 cm; range 0.5–1.2 cm) were not detected by any observer on CT but were detected on MR images by all observers. In a retrospective analysis, five HCCs were not seen on any phase of CT. Furthermore, six HCCs were poorly defined on CT, although they showed typical enhancement pattern of HCC, and the other five HCCs were clearly hypervascular on arterial phase images but showed no washout pattern.

All observers recorded 10 false-positive MRI and 5 false-positive CT results. False-positive MRI findings were attributed to three arterioportal shunts, two nodules with compact iodised oil accumulation, three dysplastic nodules (Figure 3) and two hypervascular nodules with hypointensity on hepatobiliary phase images that disappeared on follow-up imaging. Three and two false-positive CT findings were attributed to arterioportal shunts and dysplastic nodules, respectively.

All observers recorded 4 false-negative MRI and 17 false-negative CT results. In a retrospective analysis, false-negative MRI findings were attributed to two hypervascular HCCs with isointensity on hepatobiliary phase images and two HCCs <1 cm. False-negative CT findings were attributed to 14 hypervascular HCCs with no washout and 3 HCCs with poor conspicuity despite typical enhancement pattern of HCC.

The κ-values for the two observers with MRI and CT were 0.880 and 0.835, respectively, which indicates excellent interobserver agreement (Table 4).

Discussion

Our study achieved significantly higher diagnostic accuracy and sensitivity with gadoxetic acid-enhanced 3.0 T MRI than with multiphasic 64-MDCT for the detection of small (≤2 cm) HCCs in patients with chronic liver disease. One study [24] reported a higher sensitivity with gadoxetic acid-enhanced MRI using 3.0 T than by multiphasic 16- to 64-MDCT for the detection of HCCs ≤1 cm. However, the result may be inconclusive because of the small number of HCCs <1 cm. In our study, both observers found a significantly higher sensitivity with gadoxetic acid-enhanced 3.0 T MRI than with multiphasic 64-MDCT for the detection of HCCs ≤1 cm. Our study are comparable to a previous study [25] that demonstrated gadoxetic acid-enhanced MRI using 1.5 T improved the detection and characterisation of focal hepatic lesions compared with spiral CT, especially for the detection of smaller lesions or HCC underlying cirrhotic liver. We believe that the use of a liver-specific MR contrast agent may have resulted in these results. Furthermore, we think that the improved image quality of 3.0 T MRI also possibly contributed to our result. The main advantage of 3.0 T MRI compared with 1.5 T is the increase in SNR, which can be translated into higher spatial resolution and/or temporal resolution, particularly with the use of parallel imaging techniques [26, 27]. The increased effect of gadolinium at 3.0 T also contributes to increased SNR and contrast-to-noise ratio (CNR) [26, 27]. Post-gadolinium three-dimensional gradient-echo sequence at 3.0 T enables the acquisition of very high quality and thin section images, and is relatively resistant to the drawbacks of 3.0 T MRI, including specific absorption rate constraints, prolonged T_1 relaxation times and the increase in imaging artefacts [28, 29]. But there are still disadvantages with 3 T in abdominal imaging due to substantial increases in power deposition, radiofrequency field inhomogeneity, magnetic susceptibility, chemical shift artefacts and concerns regarding MR device compatibility [30]. With technical development and implementation, new applications will emerge that will improve the diagnostic capability of abdominal MRI at 3.0 T. Based on our result, the early diagnosis of HCCs <1 cm using gadoxetic acid-enhanced 3.0 T can lead to an early curative treatment by a non-surgical locoregional method such as radiofrequency ablation [4, 31, 32], with preservation of functioning liver parenchyma.

In our study, among the 59 HCCs, 16 HCCs <1.2 cm were not detected by any observer on CT. Conversely, the HCCs were detected on gadoxetic acid-enhanced MR images by all observers. We believe that although multiphasic 64-MDCT has high spatial and temporal resolution, this technique is inherently limited in the detection of small HCCs because these lesions usually have a greater chance of exhibiting poor conspicuity and atypical enhancement with no washout pattern, as in our cases.

Several investigators [10–12, 33, 34] have reported that gadoxetic acid-enhanced MRI facilitates the accurate detection and characterisation of focal liver lesions. In clinical practice, although HCCs >2 cm usually show the typical enhancement pattern (*i.e.* hypervascular at arterial phase and washout at portal or equilibrium phase) of HCC on dynamic CT or MRI, this is not always the case for HCCs <2 cm, based on previous reports [5, 35–38] and our study. Furthermore, small nodular arterial enhancing pseudolesions such as arterioportal shunt are frequently encountered in cirrhotic liver, which is a major mimicker of small HCCs. Therefore, it is important to choose the accurate imaging modality for the early diagnosis of HCCs of ≤2 cm and differentiation of small HCCs from hypervascular pseudolesions in

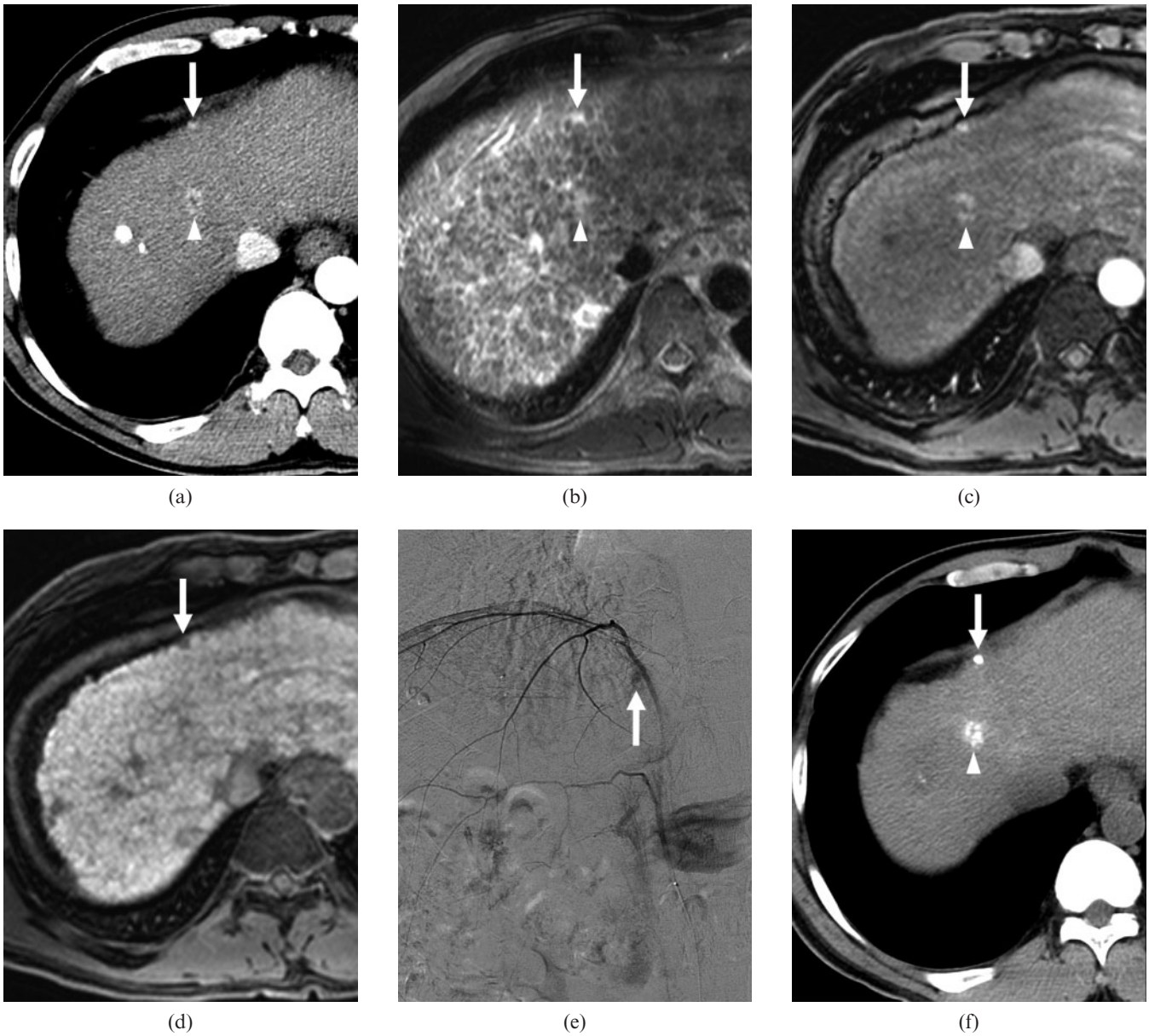

Figure 2. A 43-year-old male with a history of transcatheter arterial chemoembolisation (TACE) for hepatocellular carcinomas (HCCs) and two (1.4 and 0.6 cm in diameter) recurrent HCCs. (a) Contrast-enhanced CT scan obtained on arterial phase shows a hypervascular nodule of 1.4 cm diameter in the border of segments IV and VIII (arrowhead) and a hypervascular nodule of 0.6 cm diameter in segment IV (arrow). On contrast-enhanced CT scan obtained on equilibrium phase at same level as (a), the nodule in the border of segments IV and VIII showed a washout pattern, while the nodule in segment IV showed no washout pattern (not shown). All observers interpreted the nodule in border of segment IV and VIII as a HCC and the nodule in segment IV as arterioportal shunt. (b) T_2 weighted MR image shows two hyperintense nodules in the border of segments IV and VIII (arrowhead) as well as in segment IV (arrow). (c) Gadoxetic acid-enhanced arterial phase MR image shows two hypervascular nodules in the border of segments IV and VIII (arrowhead) and segment VI (arrow). On gadoxetic acid-enhanced 3-min late phase MR image at the same level as (c), the nodules in the border of segments IV and VIII and in segment IV showed a washout pattern (not shown). (d) Gadoxetic acid-enhanced hepatobiliary phase MR image shows two hypointense nodules in the border of segments IV and VIII (not shown) and in segment IV (arrow). All observers interpreted the two nodules as HCCs. (e) Right inferior phrenic angiography shows hypervascular tumour staining (arrow) in segment IV. The nodule in the border of segments IV and VIII also revealed hypervascular tumour staining on hepatic arteriography (not shown). (f) Unenhanced CT scan obtained after TACE shows iodised-oil accumulation at the corresponding nodules in the border of segments IV and VIII (arrowhead) and in segment IV (arrow).

clinical practice. In our study, 30% of false-positive MRI findings and 60% of false-positive CT findings are primarily attributed to an arterioportal shunt. However, none of the arterioportal shunts were hypointense on gadoxetic acid-enhanced hepatobiliary phase images in retrospective review. Previous studies [20, 39] have also shown that small (≤2 cm in diameter) HCC and hypervascular pseudolesions show different enhancing features on the hepatobiliary phase of gadoxetate acid-enhanced MRI. We believe that this finding may be helpful in differentiating the hypervascular pseudolesions, including arterioportal shunt, from small HCC. In our study, 30% of the false-positive MRI findings and 40% of the false-positive CT findings were attributed to

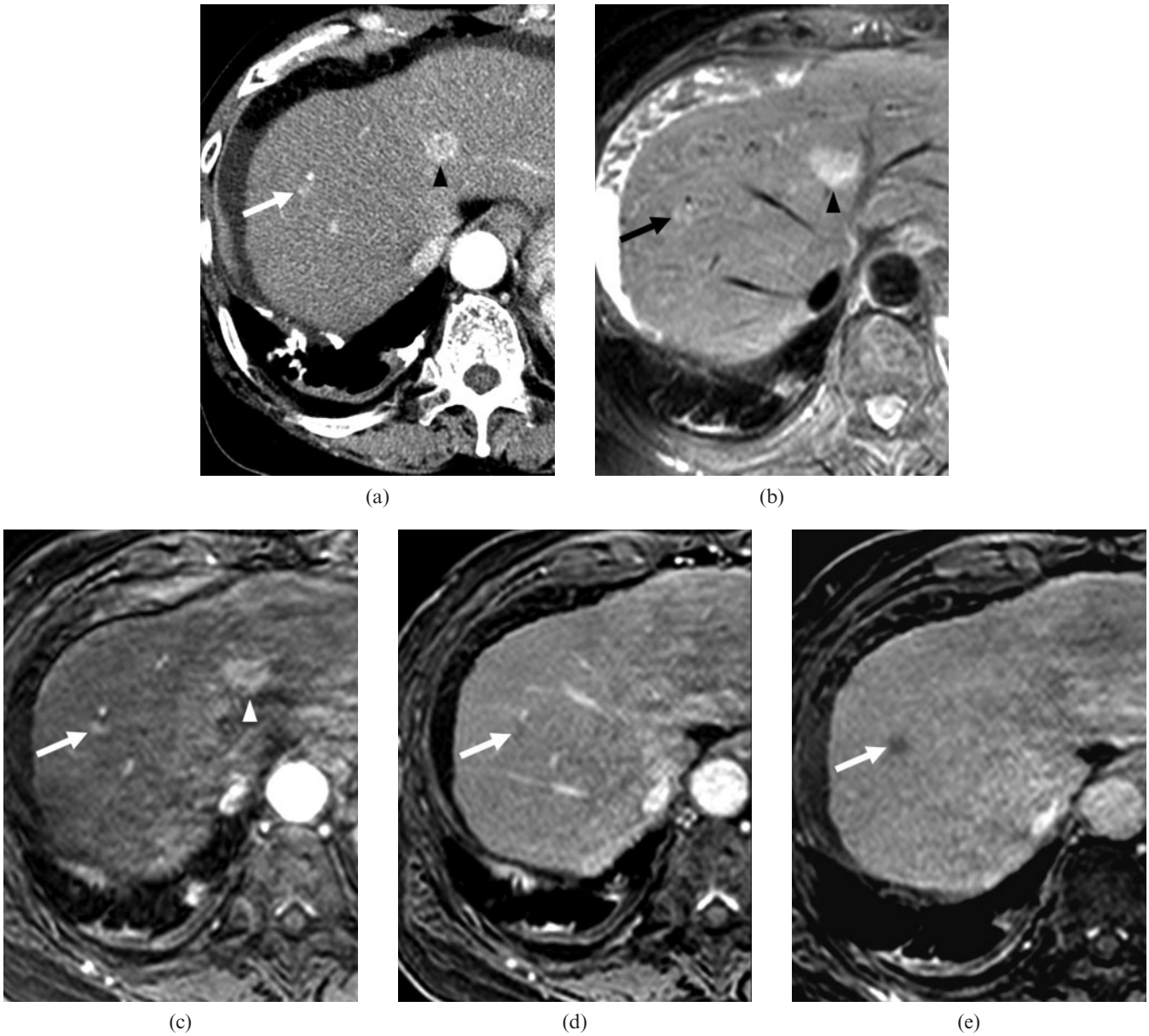

Figure 3. A 64-year-old female with a dysplastic nodule in segment VIII and a hepatocellular carcinoma (HCC) in segment IV. The lesions were confirmed by a total hepatectomy with liver transplantation. (a) Contrast-enhanced CT scan obtained on arterial phase shows a hypervascular nodule of 0.9 cm diameter (arrow) in segment VIII and a hypervascular nodule of 1.8 cm diameter in segment IV (arrowhead). On contrast-enhanced CT scan obtained on equilibrium phase at the same level as (a), the nodule in segment VIII showed no washout pattern, as opposed to the nodule in segment IV, which did show a washout pattern (not shown). All observers interpreted the nodule in segment VIII as an arterioportal shunt, and the nodule in segment IV as HCC. (b) On T_2 weighted MR image, two nodules in segments VIII (arrow) and IV (arrowhead) show hyperintensity. (c) Gadoxetic acid-enhanced arterial phase MR image shows two hypervascular nodules in segments VIII (arrow) and IV (arrowhead). (d) Gadoxetic acid-enhanced 3-min late phase MR image shows two nodules with a washout pattern in segments VIII (arrow) and IV (not shown). (e) Gadoxetic acid-enhanced hepatobiliary phase MR image shows two hypointense nodules in segments VIII (arrow) and IV (not shown). All observers interpreted two nodules as HCCs.

dysplastic nodules. Dysplastic nodules may exhibit predominant hypoattenuation on the contrast-enhanced portal or delayed phase CT images [19, 24], and might not be differentiated from hypovascular HCCs. A previous study [40] demonstrated that there was a statistically significant difference in the hypointensity on hepatobiliary phase between HCC and dysplastic nodule. Therefore, gadoxetic acid-enhanced MRI allows improved characterisation of HCC in cirrhotic liver. However, dysplastic nodules may exhibit hypervascularity in arterial phase and hypointensity in hepatobiliary phase, which might be difficult to differentiate from HCC, as in our case. In such a case, follow-up imaging is important in differentiating between the two.

Table 4. Interobserver agreement for presence of hepatocellular carcinoma

Technique	Observer 1 *vs* Observer 2
Gadoxetic acid-enhanced MRI	0.880
Multirow detector CT	0.835

Numbers are κ-values.

In our study, all of eight pathologically proven HCCs showed hypointense in the hepatocellular phase of gadoxetic acid-enhanced MRI. However, some HCCs exhibited isointensity by uptake of gadoxetic acid compared with the surrounding liver parenchyma on gadoxetic acid-enhanced hepatobiliary phase images, as in previous reports [24, 41], and may have led to false-negative results. Tsuboyama et al [42] suggested that the accumulation of gadoxetic acid in the cytoplasm of tumour cells or in the lumina of pseudoglands were induced by the expression of organic anion-transporting polypeptides 1B1 and/or -1B3 [43], which mediate the uptake of gadoxetic acid in tumour cells, as well as by either the decreased expression of multidrug resistance-associated protein 2 that mediates the secretion in tumour cells or the increased expression of MRP2 [44] at the luminal membrane of pseudoglands, which may have resulted in accumulation of gadoxetic acid in the cytoplasm of tumour cells or in the lumina of pseudoglands, regardless of the differentiation of HCCs. Therefore, based on previous studies [24, 41, 42] and our results, an isointense or hyperintense nodule with uptake of gadoxetic acid in patients with a risk of HCC on gadoxetic acid-enhanced hepatobiliary phase images may not be a benign nodule.

This study had several limitations. First, the retrospective nature of this study introduces a selection bias, although we did attempt to avoid this by only recruiting consecutive patients who met the inclusion criteria. Consequently, hypovascular HCCs, which are difficult to find in CT/MRI, were not included in our study. We consider more study to be needed with liver transplantation groups in the evaluation of atypical HCC.

Second, not all lesions were pathologically confirmed. However, acquiring pathology confirmation of all focal hepatic lesions measuring <2 cm in a cirrhotic liver would not be practical in a clinical setting. Moreover, including only those lesions that were confirmed by histopathology would have led to a verification bias, which may result in the overestimation of diagnostic predictive values. Third, in order to exclude the possibility of false-positive or false-negative results, all of the enrolled patients were followed up for more than 1 year. Nevertheless, the follow-up period may have been insufficient for the confirmative diagnosis.

In conclusion, gadoxetic acid-enhanced 3.0 T MRI showed a better diagnostic performance than the multiphasic 64-MDCT for the detection of small (≤ 2 cm) HCCs in patients with chronic liver disease.

References

1. Benvegnu L, Gios M, Boccato S, Alberti A. Natural history of compensated viral cirrhosis: a prospective study on the incidence and hierarchy of major complications. Gut 2004; 53:744–9.
2. Bosch FX, Ribes J, Diaz M, Cleries R. Primary liver cancer: worldwide incidence and trends. Gastroenterology 2004; 127:S5–16.
3. Forner A, Vilana R, Ayuso C, Bianchi L, Sole M, Ayuso JR, et al. Diagnosis of hepatic nodules 20 mm or smaller in cirrhosis: prospective validation of the noninvasive diagnostic criteria for hepatocellular carcinoma. Hepatology 2008;47: 97–104.
4. Bruix J, Sherman M. Management of hepatocellular carcinoma. Hepatology 2005;42:1208–36.
5. Willatt JM, Hussain HK, Adusumilli S, Marrero JA. MR Imaging of hepatocellular carcinoma in the cirrhotic liver: challenges and controversies. Radiology 2008;247:311–30.
6. Kopp AF, Heuschmid M, Claussen CD. Multidetector helical CT of the liver for tumor detection and characterization. Eur Radiol 2002;12:745–52.
7. Iannaccone R, Laghi A, Catalano C, Rossi P, Mangiapane F, Murakami T, et al. Hepatocellular carcinoma: role of unenhanced and delayed phase multi-detector row helical CT in patients with cirrhosis. Radiology 2005;234:460–7.
8. Zech CJ, Vos B, Nordell A, Urich M, Blomqvist L, Breuer J, et al. Vascular enhancement in early dynamic liver MR imaging in an animal model: comparison of two injection regimen and two different doses Gd-EOB-DTPA (gadoxetic acid) with standard Gd-DTPA. Invest Radiol 2009;44: 305–10.
9. Yoon MA, Kim SH, Park HS, Lee DH, Lee JY, Han JK, et al. Value of dual contrast liver MRI at 3.0 T in differentiating well-differentiated hepatocellular carcinomas from dysplastic nodules: preliminary results of multivariate analysis. Invest Radiol 2009;44:641–9.
10. Bartolozzi C, Crocetti L, Lencioni R, Cioni D, Della Pina C, Campani D. Biliary and reticuloendothelial impairment in hepatocarcinogenesis: the diagnostic role of tissue-specific MR contrast media. Eur Radiol 2007;17:2519–30.
11. Huppertz A, Balzer T, Blakeborough A, Breuer J, Giovagnoni A, Heinz-Peer G, et al. Improved detection of focal liver lesions at MR imaging: multicenter comparison of gadoxetic acid-enhanced MR images with intraoperative findings. Radiology 2004;230:266–75.
12. Halavaara J, Breuer J, Ayuso C, Balzer T, Bellin MF, Blomqvist L, et al. Liver tumor characterization: comparison between liver-specific gadoxetic acid disodium-enhanced MRI and biphasic CT—a multicenter trial. J Comput Assist Tomogr 2006;30:345–54.
13. Park Y, Kim SH, Jeon YH, Lee J, Kim MJ, Choi D, et al. Gadoxetic acid (Gd-EOB-DTPA)-enhanced MRI versus gadobenate dimeglumine (Gd-BOPTA)-enhanced MRI for preoperatively detecting hepatocellular carcinoma: an initial experience. Korean J Radiol 2010;11:433–40.
14. Semelka RC, Martin DR, Balci C, Lance T. Focal liver lesions: comparison of dual-phase CT and multisequence multiplanar MR imaging including dynamic gadolinium enhancement. J Magn Reson Imaging 2001;13:397–401.
15. Hussain SM, Semelka RC. Hepatic imaging: comparison of modalities. Radiol Clin North Am 2005;43:929–47.
16. Baron RL, Oliver JH 3rd, Dodd GD 3rd, Nalesnik M, Holbert BL, Carr B. Hepatocellular carcinoma: evaluation with biphasic, contrast-enhanced, helical CT. Radiology 1996;199:505–11.
17. Jang HJ, Lim JH, Lee SJ, Park CK, Park HS, Do YS. Hepatocellular carcinoma: are combined CT during arterial portography and CT hepatic arteriography in addition to triple-phase helical CT all necessary for preoperative evaluation? Radiology 2000;215:373–80.
18. Kang BK, Lim JH, Kim SH, Choi D, Lim HK, Lee WJ, et al. Preoperative depiction of hepatocellular carcinoma: ferumoxides-enhanced MR imaging versus triple-phase helical CT. Radiology 2003;226:79–85.
19. Kim SH, Choi D, Lim JH, Lee WJ, Kim MJ, Lim HK, et al. Ferucarbotran-enhanced MRI versus triple-phase MDCT for the preoperative detection of hepatocellular carcinoma. AJR Am J Roentgenol 2005;184:1069–76.
20. Sun HY, Lee JM, Shin CI, Lee DH, Moon SK, Kim KW, et al. Gadoxetic acid-enhanced magnetic resonance imaging for differentiating small hepatocellular carcinomas (< or =2 cm in diameter) from arterial enhancing pseudolesions:

special emphasis on hepatobiliary phase imaging. Invest Radiol 2010;45:96–103.
21. Hanley JA, McNeil BJ. A method of comparing the areas under receiver operating characteristic curves derived from the same cases. Radiology 1983;148:839–43.
22. Bennett BM. On comparisons of sensitivity, specificity and predictive value of a number of diagnostic procedures. Biometrics 1972;28:793–800.
23. Landis JR, Koch GG. The measurement of observer agreement for categorical data. Biometrics 1977;33:159–74.
24. Kim SH, Lee J, Kim MJ, Jeon YH, Park Y, Choi D, et al. Gadoxetic acid-enhanced MRI versus triple-phase MDCT for the preoperative detection of hepatocellular carcinoma. AJR Am J Roentgenol 2009;192:1675–81.
25. Ichikawa T, Saito K, Yoshioka N, Tanimoto A, Gokan T, Takehara Y, et al. Detection and characterization of focal liver lesions: a Japanese phase III, multicenter comparison between gadoxetic acid disodium-enhanced magnetic resonance imaging and contrast-enhanced computed tomography predominantly in patients with hepatocellular carcinoma and chronic liver disease. Invest Radiol 2010;45:133–41.
26. Akisik FM, Sandrasegaran K, Aisen AM, Lin C, Lall C. Abdominal MR imaging at 3.0 T. Radiographics 2007;27: 1433–44.
27. Barth MM, Smith MP, Pedrosa I, Lenkinski RE, Rofsky NM. Body MR imaging at 3.0 T: understanding the opportunities and challenges. Radiographics 2007;27:1445–62.
28. Zapparoli M, Semelka RC, Altun E, Tsurusaki M, Pamuklar E, Dale BM, et al. 3.0-T MRI evaluation of patients with chronic liver diseases: initial observations. Magn Reson Imaging 2008;26:650–60.
29. Ramalho M, Altun E, Heredia V, Zapparoli M, Semelka R. Liver MR imaging: 1.5 T versus 3 T. Magn Reson Imaging Clin N Am 2007;15:321–47.
30. Chang KJ, Kamel IR, Macura KJ, Bluemke DA. 3.0-T MR imaging of the abdomen: comparison with 1.5 T. Radiographics 2008;28:1983–98.
31. Sherman M. Diagnosis of small hepatocellular carcinoma. Hepatology 2005;42:14–16.
32. Llovet JM, Burroughs A, Bruix J. Hepatocellular carcinoma. Lancet 2003;362:1907–17.
33. Hammerstingl R, Huppertz A, Breuer J, Balzer T, Blakeborough A, Carter R, et al. Diagnostic efficacy of gadoxetic acid (Primovist)-enhanced MRI and spiral CT for a therapeutic strategy: comparison with intraoperative and histopathologic findings in focal liver lesions. Eur Radiol 2008;18:457–67.
34. Vogl TJ, Kummel S, Hammerstingl R, Schellenbeck M, Schumacher G, Balzer T, et al. Liver tumors: comparison of MR imaging with Gd-EOB-DTPA and Gd-DTPA. Radiology 1996;200:59–67.
35. Bolondi L, Gaiani S, Celli N, Golfieri R, Grigioni WF, Leoni S, et al. Characterization of small nodules in cirrhosis by assessment of vascularity: the problem of hypovascular hepatocellular carcinoma. Hepatology 2005;42:27–34.
36. Jeong YY, Mitchell DG, Kamishima T. Small (<20 mm) enhancing hepatic nodules seen on arterial phase MR imaging of the cirrhotic liver: clinical implications. AJR Am J Roentgenol 2002;178:1327–34.
37. Yu JS, Chung JJ, Kim JH, Kim KW. Small hypervascular hepatocellular carcinomas: value of ''washout'' on gadolinium-enhanced dynamic MR imaging compared to superparamagnetic iron oxide-enhanced imaging. Eur Radiol 2009;19:2614–22.
38. Yoon SH, Lee JM, So YH, Hong SH, Kim SJ, Han JK, et al. Multiphasic MDCT enhancement pattern of hepatocellular carcinoma smaller than 3 cm in diameter: tumor size and cellular differentiation. AJR Am J Roentgenol 2009;193: W482–9.
39. Motosugi U, Ichikawa T, Sou H, Sano K, Tominaga L, Muhi A, et al. Distinguishing hypervascular pseudolesions of the liver from hypervascular hepatocellular carcinomas with gadoxetic acid-enhanced MR imaging. Radiology 2010;256: 151–8.
40. Kim JI, Lee JM, Choi JY, Kim YK, Kim SH, Lee JY, et al. The value of gadobenate dimeglumine-enhanced delayed phase MR imaging for characterization of hepatocellular nodules in the cirrhotic liver. Invest Radiol 2008;43:202–10.
41. Huppertz A, Haraida S, Kraus A, Zech CJ, Scheidler J, Breuer J, et al. Enhancement of focal liver lesions at gadoxetic acid-enhanced MR imaging: correlation with histopathologic findings and spiral CT—initial observations. Radiology 2005;234:468–78.
42. Tsuboyama T, Onishi H, Kim T, Akita H, Hori M, Tatsumi M, et al. Hepatocellular carcinoma: hepatocyte-selective enhancement at gadoxetic acid-enhanced MR imaging—correlation with expression of sinusoidal and canalicular transporters and bile accumulation. Radiology 2010;255: 824–33.
43. Konig J, Cui Y, Nies AT, Keppler D. Localization and genomic organization of a new hepatocellular organic anion transporting polypeptide. J Biol Chem 2000;275:23161–8.
44. Nies AT, Konig J, Pfannschmidt M, Klar E, Hofmann WJ, Keppler D. Expression of the multidrug resistance proteins MRP2 and MRP3 in human hepatocellular carcinoma. Int J Cancer 2001;94:492–9.